Proceedings of the Twentieth (2010) International Offshore and Polar Engineering Conference
Beijing, China, June 20–25, 2010

ISBN 978-1-880653-77-7 (Set); ISSN 1098-6189 (Set); www.isope.org

Modeling of Fully Nonlinear Wave Interactions with Moving Submerged Structures

Etienne Guerber [1], Michel Benoit [1], Stéphan T. Grilli [2], Clément Buvat [1]

[1]Saint-Venant Laboratory for Hydraulics
Université Paris-Est
Chatou, France

[2]Department of Ocean Engineering
University of Rhode Island
Narragansett, RI, USA

ABSTRACT

The purpose of this work is to develop advanced numerical tools for modeling two-way fully nonlinear interactions of ocean surface waves (irregular waves in the general situation) with a submerged structure undergoing large amplitude motion. The final aim is to apply these models to simulating the behavior of a point-absorber-type Wave Energy Converter (WEC). In our modeling approach, an existing two-dimensional Numerical Wave Tank (NWT), based on potential flow theory, is extended to include a submerged horizontal cylinder of arbitrary cross-section. The mathematical problem and related numerical solution are first introduced. Then we present two applications, first for the prescribed motion of a submerged body in a wave field (including the case of a fixed cylinder, such as in Chaplin's (1984) experiments), and then for a freely-moving body in waves. In the first application, we consider the forced oscillations of a circular cylinder, either in the vertical direction or in a circular motion (with comparison to the theoretical results of Wu (1993)). In the second application, dynamical equations describing the body motion are solved simultaneously with the hydrodynamic problem, which requires correctly representing the coupling forces between both mechanical and hydrodynamic problems. This is illustrated by preliminary simulations for the free motion in periodic waves of an idealized WEC; these results are favorably compared to a linear model.

KEY WORDS: Numerical wave tank; fluid-structure interactions; wave-energy converter.

INTRODUCTION

In recent years there has been a renewed interest in using ocean renewable energy and, in particular, wave energy. To do so, many types of Wave Energy Converters (WECs) have been proposed, and some constructed and tested. Some types of so-called point-absorber WEC are based on harvesting the wave-induced motion of oscillating submerged bodies (see, e.g., the CETO system; Mann et al., 2007). These bodies can be quite close to the free surface and may undergo large amplitude motion. In these situations numerical models based on assuming small amplitude motions, either of the free surface waves, the body dynamics, or both, may not properly represent the dynamics of the coupled system. In the present study we aim at developing a numerical model solving two-way nonlinear body-wave interactions, which could then be applied to simulating WEC behavior in real (irregular) sea-states. As a first step in this project, we implement and validate a two-dimensional (2D) model for a horizontal submerged cylinder. Many papers have been dedicated to the analytical and experimental study of the nonlinear response of such submerged circular cylinders. Chaplin (1984), for instance, experimentally studied in a wave tank the influence of the Keulegan-Carpenter number on the nonlinear wave force exerted on a fixed submerged cylinder. More recently, Wu (1993) formulated a mathematical model to calculate the forces exerted on a submerged cylinder undergoing large-amplitude motions. The body-surface condition is satisfied on its instantaneous position while the free surface condition is linearized. The solution for the potential is expressed in terms of a multipole expansion. In particular, Wu obtained results for a circular cylinder in prescribed motion in a wave field: purely vertical motion and clock-wise circular motion (Wu, 1993). Such studies were later used to validate results of numerical models based on potential flow theory. Among others, Cointe (1989) compared numerical results from the fully nonlinear model *Sindbad* to Chaplin's experiments. Kent and Choi (2007), using the High-Order Spectral Method (HOS), compared their results to both Wu's theory and Chaplin's experiments.

The numerical simulations reported here are performed using a Fully Nonlinear Potential Flow (FNPF) model, applied to simulating strongly nonlinear interactions (i.e., induced motion and forces) between wave-induced flows and a submerged body representing a WEC section, slackly moored on the ocean bottom. The present model is an extension of Grilli et al.'s two-dimensional (2D) FNPF Boundary Element Model (BEM), which was developed over the past 20 years to simulate processes of wave generation, propagation and interaction with structures, and dissipation through breaking or absorption in a numerical beach (e.g., Grilli et al., 1989; Grilli and Subramanya, 1996; Grilli and Horrillo, 1997). The latter processes take place both in the field and laboratory tanks; this has led such models to be referred to as Numerical Wave Tanks (NWTs).

In our particular implementation, second-order Taylor series expansions are expressed, in an Eulerian-Lagrangian formulation, for

the time updating of the free surface potential, the free surface position, and an absorbing wavemaker at the far end of the NWT. This requires solving two elliptic problems at each time step, one for the potential and one for its time derivative (the latter allows for a straightforward calculation of pressure on all boundaries, including that of the submerged structure/WEC).

Higher-order elements and very accurate numerical integration methods are used in the BEM that allow to achieve extremely high accuracy of the solution and thus to perform long term simulations without need for smoothing or filtering of the solution. An absorbing beach combining an "absorbing pressure" on the free surface and a lateral absorbing piston wavemaker allows to achieve negligible reflection in the NWT. Various ways of generating waves are available, including flap and piston wavemakers, exact nonlinear waves (both periodic and solitary), and internal sources. Wavemakers can also be used to generate nonlinear random waves based on standard energy spectra specified on input. A feedback control loop allows to iteratively modify the wavemaker stroke spectrum to better approach the targeted wave spectrum. While random waves can be generated, the present work, which is preliminary, focuses on nonlinear interactions of a cylindrical structure with monochromatic periodic waves.

MATHEMATICAL FORMULATION

Overview of the NWT

Equations for the two-dimensional FNPF model are briefly presented in the following (see, Grilli et al., 1989; Grilli and Svendsen, 1990; Grilli and Subramanya, 1996; Grilli and Horrillo, 1997 for details). The velocity potential is used to describe inviscid irrotational flows in the vertical plane (x, z) and the velocity is defined by $\mathbf{u} = \nabla\phi = (u, w)$.

Continuity equation in the fluid domain $\Omega(t)$ with boundary $\Gamma(t)$ is a Laplace's equation for the potential (Fig. 1),

$$\nabla^2\phi = 0 \qquad \text{in } \Omega(t) \tag{1}$$

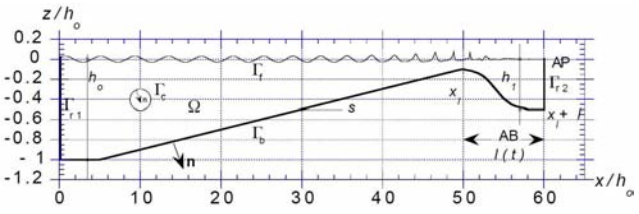

Figure 1: Sketch of computational domain Ω and its boundaries.

On the free surface $\Gamma_f(t)$, ϕ satisfies the kinematic and dynamic boundary conditions,

$$\frac{D\mathbf{r}}{Dt} = \left(\frac{\partial}{\partial t} + \mathbf{u}\cdot\nabla\right)\mathbf{r} = \mathbf{u} = \nabla\phi \qquad \text{on } \Gamma_f(t) \tag{2}$$

$$\frac{D\phi}{Dt} = -gz + \frac{1}{2}\nabla\phi\cdot\nabla\phi - \frac{p_a}{\rho} \qquad \text{on } \Gamma_f(t) \tag{3}$$

respectively, with $\mathbf{r}$, the position vector on the free surface, g the gravitational acceleration, z the vertical coordinate, p_a the pressure at the free surface, and ρ the fluid density. Along the stationary bottom Γ_b, the no-flow condition is prescribed as,

$$\frac{\partial\phi}{\partial n} = 0 \qquad \text{on } \Gamma_b \tag{4}$$

On the leftward boundary of the NWT, Γ_{r1} , periodic or irregular waves are generated by an oscillating piston or flap wavemaker. An exact wave generation for periodic progressive waves based on the stream-function wave theory can also be specified, with a zero-mass flux condition. On the rightward side of the tank, an absorbing beach (AB) is implemented to reduce wave reflection from the far end boundary Γ_{r2}. Thus, an artificial counteracting pressure is applied over a given distance in the dynamic free surface condition (Eq. 3), which creates a negative work against incident waves. In addition, a piston-like absorbing boundary condition, first introduced by Clément (1996), is specified on boundary Γ_{r2}. Details about generation and absorption of waves in the model can be found in Grilli and Horrillo (1997). A specific boundary condition is applied on the rigid body boundary Γ_c, depending on whether the body is moving in a prescribed motion or not. This condition will be described in the next section.

Eq. 1 is transformed into a Boundary Integral Equation (BIE), using Green's second identity, and solved by a BEM. The BIE is thus evaluated at N nodes on the boundary and M higher-order elements are defined to interpolate in between discretization nodes. In the present applications, quadratic isoparametric elements are used on lateral and bottom boundaries. Isoparametric linear elements are used on the body boundary and cubic elements on the free surface in order to ensure continuity of the boundary slope. In these latter elements, referred to as Mixed Cubic Interpolation (MCI) elements, geometry is modeled by cubic splines and field variables are interpolated between each pair of nodes, using the mid-section of a four-node "sliding" isoparametric element. Quadratic isoparametric elements are currently being tested on the body boundary and corresponding results should be presented at the conference. Expressions of BEM integrals (regular, singular, quasi-singular) are given in Grilli et al. (1989), Grilli and Svendsen (1990), and Grilli and Subramanya (1994, 1996), for isoparametric and MCI elements.

Free surface boundary conditions (Eqs. 2 and 3) are marched in time based on two second-order Taylor series expansions expressed in terms of a time step Δt and of the Lagrangian time derivative, D/Dt, for ϕ and $\mathbf{r}$. First-order coefficients in the series correspond to free surface conditions (Eqs. 2 and 3), in which ϕ and $\partial\phi/\partial n$ are obtained from the solution of the BIE for $(\phi, \partial\phi/\partial n)$ at time t. Second-order coefficients are expressed as D/Dt of Eqs. 2 and 3, and calculated using the solution of a second BIE for $(\partial\phi/\partial t, \partial^2\phi/\partial t\partial n)$, for which boundary conditions are obtained from the solution of the first problem. Detailed expressions for the Taylor series are given in Grilli et al. (1989). A detailed account of the 2D-FNPF and review of applications to date can also be found in Grilli (1997).

This two-dimensional NWT was recently modified to take into account the presence of a rigid body totally submerged under the free surface. Two situations are successively considered: (i) the case of a body in prescribed motion (including the case of a fixed body); and (ii) the case of a body undergoing "free" motion (under the effects of various forces applied to it).

Body in Prescribed Motion

When the body motion is specified, the boundary condition on the body surface is simply expressed as a Neumann condition for the potential:

$$\frac{\partial\phi}{\partial n} = \dot{\alpha}\cdot\mathbf{n} \qquad \text{on } \Gamma_c \tag{5}$$

where $\dot{\alpha}$ is the velocity of points on the body boundary, which is known when the motion of the body is prescribed.
Since a second BIE is solved for ($\partial\phi/\partial t$, $\partial^2\phi/\partial t\partial n$), another condition is needed to solve for $\partial\phi/\partial t$. Following Cointe (1989), Grilli and Svendsen (1990), Van Daalen (1993), or Tanizawa (1995), a Neumann condition on $\partial^2\phi/\partial t\partial n$ is imposed at the body boundary:

$$\frac{\partial^2\phi}{\partial t\partial n} = \ddot{\alpha}\cdot\mathbf{n} + \dot{\theta}\left(\dot{\alpha}\cdot\mathbf{s} - \frac{\partial\phi}{\partial s}\right) - \left(\frac{1}{R}\frac{\partial\phi}{\partial s} + \frac{\partial^2\phi}{\partial s\partial n}\right)\dot{\alpha}\cdot\mathbf{s} + \left(\frac{\partial^2\phi}{\partial s^2} - \frac{1}{R}\frac{\partial\phi}{\partial n}\right)\dot{\alpha}\cdot\mathbf{n} \qquad \text{on } \Gamma_c \quad (6)$$

where, $\ddot{\alpha}, \dot{\theta}$ are respectively the solid acceleration of the point of the body boundary and the rotational velocity of the body. $1/R$ is the local curvature of the boundary. **n** and **s** are the local normal and tangential vectors. Those conditions (Eqs. 5 and 6) are similar to the conditions imposed for the generation of waves by a flap wavemaker (Grilli and Horrillo, 1997; Grilli, 1997). Various results are presented in a following section for a submerged circular cylinder in purely vertical motion and then in circular motion in a wave field.

Freely Moving Body

When no motion is imposed to the body, the problem to be solved is referred to as a *freely-moving body* problem. In this case, the acceleration $\ddot{\alpha}$ is not *a priori* known, which implies that Eq. 6 cannot directly be used as a boundary condition to solve the Laplace problem for $\partial\phi/\partial t$. Furthermore, $\dot{\alpha}$ in Eq. 5 needs to be solved as part of a coupled fluid-structure problem in which equations for the fluid motion must be solved in combination with those for the rigid body motion.

Assuming a body of mass M and mass moment of inertia I about its center of mass, the dynamic equations governing the body motion read:

$$M\ddot{\mathbf{x}} = \int_{\Gamma_c} p\mathbf{n}d\Gamma - Mg\underline{\mathbf{z}} + \mathbf{F}_{ext} \quad (7)$$

$$I\ddot{\theta}\underline{\mathbf{y}} = \int_{\Gamma_c} p(\mathbf{r}\times\mathbf{n})d\Gamma \quad (8)$$

In Eq. 7, $\ddot{\mathbf{x}}$ is the body center of mass acceleration, $\ddot{\theta}$ is the solid body angular acceleration about the center of mass, $\mathbf{F}_{ext}$ represents any kind of applied external force that essentially damp the body motion (e.g., mooring, power take-off...), **r** is the position of a point on the body boundary with respect to the center of mass and $\underline{\mathbf{z}}$ is the vertical upward unit vector. Finally, pressure p along the body boundary is given by the (nonlinear) Bernoulli equation:

$$p = -\rho\left(\frac{\partial\phi}{\partial t} + \frac{1}{2}\nabla\phi\cdot\nabla\phi + gz\right) \quad (9)$$

The main difficulty for computing this pressure is that both $\partial\phi/\partial t$ and $\partial^2\phi/\partial t\partial n$ are unknown at any given time along Γ_c, since these depend on the body motion. Several strategies have been proposed to overcome this: (i) a mode decomposition method first proposed by Vinje and Brevig (1981) and then used by Cointe (1989) and Koo and Kim (2004); (ii) the iterative method by Sen (1993) and Cao et al. (1994); (iii) the indirect method by Wu and Eatock-Taylor (1996); and (iv) the implicit method by Van Daalen (1993) and Tanizawa (1995). The implicit method is selected here, as no iterations are required and there is no need to introduce any artificial potential. In this method, we use the integral relationship between $\partial\phi/\partial t$ and $\partial^2\phi/\partial t\partial n$ on Γ_c, derived by Van Daalen (1993) and Tanizawa (1995) based on Eqs. 7~9:

$$\frac{\partial^2\phi}{\partial t\partial n}(\mathbf{x}) + \int_{\Gamma_c} K(\mathbf{x},\xi)\frac{\partial\phi}{\partial t}(\xi)d\Gamma_\xi = \gamma(\mathbf{x}) \quad (10)$$

in which the kernel function $K(\mathbf{x},\xi)$ is regular and symmetric, and only depends on the body geometry (i.e., is valid for all times):

$$K(\mathbf{x},\xi) = \frac{1}{M}\mathbf{n}(\mathbf{x})\cdot\mathbf{n}(\xi) + \frac{1}{I}\{\mathbf{r}(\mathbf{x})\times\mathbf{n}(\mathbf{x})\}\cdot\{\mathbf{r}(\xi)\times\mathbf{n}(\xi)\} \quad (11)$$

For 2D problems, we further express $\gamma(\mathbf{x})$ as:

$$\gamma(\mathbf{x}) = -\int_{\Gamma_c}\left\{\frac{1}{2}\nabla\phi(\xi)\cdot\nabla\phi(\xi) + gz(\xi)\right\}K(\mathbf{x},\xi)d\Gamma_\xi - \dot{\theta}^2\mathbf{r}(\mathbf{x})\cdot\mathbf{n}(\mathbf{x}) + \nu - g\underline{\mathbf{z}}\cdot\mathbf{n}(\mathbf{x}) - \frac{1}{M}\mathbf{F}_{ext}\cdot\mathbf{n}(\mathbf{x}) \quad (12)$$

with ν a local quantity defined as:

$$\nu = \dot{\theta}\left(\dot{\alpha}\cdot\mathbf{s} - \frac{\partial\phi}{\partial s}\right) - \left(\frac{1}{R}\frac{\partial\phi}{\partial s} + \frac{\partial^2\phi}{\partial s\partial n}\right)\dot{\alpha}\cdot\mathbf{s} \quad (13)$$

Eq. 10 provides an extra BIE, which is discretized on the body boundary Γ_c using the BEM elements. Following Van Daalen (1993), at any given time, after solving for ϕ, the extra BIE (Eq. 10) is added to the matrix of the second BIE problem for $\partial\phi/\partial t$, so that the number of equations equals the number of unknowns. The new linear system is solved using the direct Kaletsky elimination technique (Grilli et al., 1989). Eqs. 7 and 8 are then time-integrated, and the position and velocity of the body center of mass are updated to the next time step. Various schemes have been considered and compared for simplified model equations (mechanical oscillator). Based on these tests, a Newmark scheme was retained (given here for Eq. 7):

$$\dot{\mathbf{x}}_{n+1} = \dot{\mathbf{x}}_n + \Delta t\left[(1-\gamma)\ddot{\mathbf{x}}_n + \gamma\ddot{\mathbf{x}}_{n+1}\right] \quad (14)$$

$$\mathbf{x}_{n+1} = \mathbf{x}_n + \Delta t\dot{\mathbf{x}}_n + \Delta t^2\left[(\frac{1}{2}-\beta)\ddot{\mathbf{x}}_n + \beta\ddot{\mathbf{x}}_{n+1}\right] \quad (15)$$

Parameters were selected as $\gamma = 1/2$ and $\beta = 1/12$, corresponding to the so-called Fox-Goodwin method (1949). As this scheme is implicit ($\ddot{\mathbf{x}}_{n+1}$ is unknown), iterations are required. As initial values, we used time extrapolations based on the values of the unknown quantities at the two previous time steps. Note, time step is fixed by the hydrodynamic solver.

FIXED CYLINDER BENEATH WAVES

Significant research was devoted to analyzing diffraction around a submerged fixed cylinder. Thus Dean (1948), using a linearized potential theory, showed that there is no reflection of incident waves by the cylinder, and that transmitted waves only undergo a phase shift when passing the obstacle. Ursell (1949) and later Ogilvie (1963) extended the formulation up to the second order in wave steepness.

Chaplin (1984) experimentally measured the nonlinear force on a horizontal fixed cylinder beneath waves in a wave flume. In particular he analyzed the influence of the Keulegan-Carpenter number on the harmonics of the applied force, with:

$$K_c = \frac{\pi H}{2R} e^{kz_c} = \frac{\pi A}{R} e^{kz_c} \tag{16}$$

where $H = 2A$ is the wave height, R the cylinder radius, k the wave number, and z_c the cylinder submergence. Chaplin's results were in good agreement with Ogilvie' s theory when the wave steepness was low, but important nonlinear effects were experimentally observed for higher steepness. Grue and Granlund (1988) also conducted some experiments, focusing on the diffracted waves.

Numerical tests were conducted with the present NWT and the computed hydrodynamic forces compared to Chaplin's results for case E. Waves are generated using the stream-function wave method in a flume of water depth $d = 0.85$ m and length $L = 29.6$ m; an absorbing beach is implemented over the last 7 m. The wave period is $T = 1$ s and the wave height is progressively increased from 0.0018 m to 0.0720 m. The cylinder of radius $R = 0.051$ m is placed 8 m away from the wavemaker, at $z_c = -0.102$ m under the undisturbed free surface.

In the BEM, 350 nodes are used on the free surface, and 25 on the cylinder boundary. Following Chaplin, the non-dimensional vertical F_z and horizontal F_x forces are written as Fourier series and the amplitudes of the harmonics are computed with a FFT over the last 3 periods of the simulations:

$$\frac{F_x}{\rho R^3 \omega^2} = F_x^{(0)} + \sum_{n\geq 1} F_x^{(n)} \cos(n\omega t + \psi^{(n)}) \tag{17}$$

$$\frac{F_z}{\rho R^3 \omega^2} = F_z^{(0)} + \sum_{n\geq 1} F_z^{(n)} \sin(n\omega t + \psi^{(n)}) \tag{18}$$

Fig. 2 shows a good agreement of the mean vertical force with both Chaplin' s experimental results and Ogilvie' s second-order theory. However, the first harmonics (Fig. 3) only agrees with Chaplin's measurements at the lower values of K_c.
At larger values, the decrease of the experimental first-order coefficient is not reproduced by the model, likely due to viscous effects and the recirculation created around the body (Chaplin, 1984). This is confirmed by Tavassoli and Kim's (2001) simulations, performed in a viscous NWT, who did obtain the experimental decrease. Some of their results are presented on Fig. 3.

The second and third harmonics were also computed (Fig. 4) with a good general agreement with measurements. A slight discrepancy is observed at larger values of K_c, which can also be attributed to viscous effects, as also shown by the model results of Tavassoli and Kim (2001). Note, in these simulations, no saw-tooth instabilities of the free surface nor breaking of waves passing over the cylinder were observed.
The results computed by the present model are in good agreement with Chaplin's results up to the point where viscous effects play a significant role. Other numerical studies based on potential theory were compared to Chaplin's experiments without any better agreement: e.g. Liu et al. (1992) and Kent and Choi (2007) using a HOS method, Cointe (1989) and Koo and Kim (2003) using a BEM. This confirms the ability of the present model to reproduce nonlinear wave interactions with a structure, submerged quite close to the free surface.

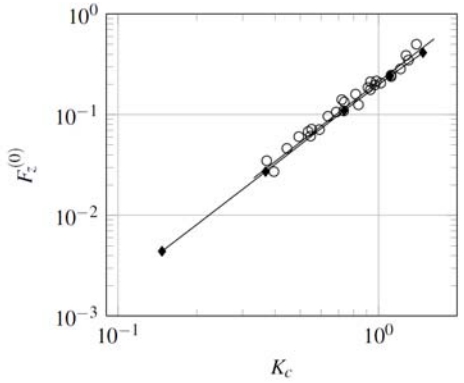

Figure 2: Adimensioned Mean Vertical Force - NWT results (—♦—) compared to Chaplin's (1984) experiments (○) and to 2nd order theory of Ogilvie (1963) (——).

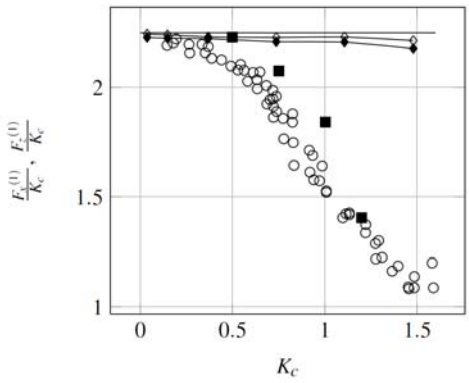

Figure 3: 1st harmonic of the horizontal (—♦—) and vertical force (—◇—) compared to Chaplin's (1984) experiments (○), linear theory of Ogilvie (1963) (——) and viscous simulations of Tavassoli and Kim (2001) (■).

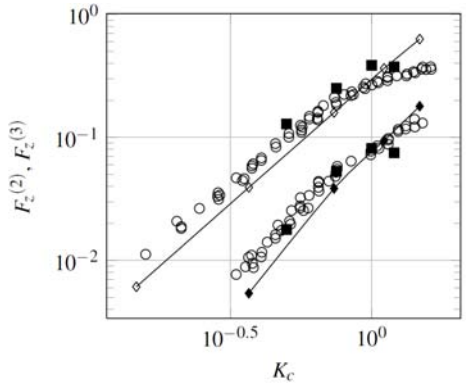

Figure 4: 2nd (—◇—) and 3rd (—♦—) harmonics of the adimensioned vertical force compared to Chaplin's (1984) experiments (○) and viscous simulations of Tavassoli and Kim (2001) (■).

A SUBMERGED CYLINDER WITH PRESCRIBED MOTION

Cylinder in a Prescribed Purely Vertical Motion

The radiation problem of a submerged circular cylinder undertaking large amplitude motion in still water was analytically solved by Wu (1993), with no approximation on the cylinder boundary condition but linearized free surface conditions. Wu wrote the potential in terms of a multipole expansion and computed the vertical hydrodynamic force exerted on a cylinder (radius R) in purely vertical motion, for two non-dimensional wave numbers ($kR = 0.1$) and ($kR = 1.0$) and 8 amplitudes of motion B/R. The wave number of waves generated by the cylinder oscillations was related to the frequency of motion, as predicted by the linear dispersion relation in infinite depth $k = \omega^2/g$.

Wu also decomposed the non-dimensional vertical force in a Fourier series:

$$\frac{F_z}{\rho B \pi R^2 \omega^2} = F_z^{(0)} + \sum_{n\geq 1} F_z^{(n)} \sin(n\omega t + \psi^{(n)}) \qquad (19)$$

Our numerical simulations for this case were run in a flume of water depth $d = 3$ m and length $L = 20$ m, with an absorbing beach over the last 7 m. A cylinder of radius $R = 0.1$ m is placed 10 m away from the wavemaker and $z_c = -3R$ under the undisturbed free surface (mean position) and is vertically moved with oscillations of angular frequency ω and amplitude B. A two period ramp-up is specified to gradually reach steady-state, to prevent instabilities that could occur with an impulsive start. The hypothesis of infinite depth made by Wu was approximately verified in our simulations, with $kd = 3$ for the first frequency of oscillations ($kR = 0.1$) and $kd = 30$ for the second one ($kR = 1.0$). For both frequencies, in the BEM, 200 nodes were used on the free surface and 80 on the cylinder; simulations lasted for about 10 periods. In the model, starting from a free-surface at rest, the motion of the cylinder induces the generation and propagation of symmetric waves in both leftward and rightward directions (Fig. 5), as was observed in experiments.

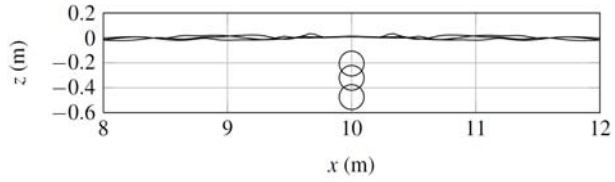

Figure 5: Successive snapshots ($t/T = 2.75$, $t/T = 2.99$, $t/T = 3.10$) of waves generated by the forced purely vertical motion of a cylinder ($B/R = 1.75$, $kR = 0.1$)

A Fourier analysis was applied to results for the last period of simulations. Fig. 6 presents the mean hydrodynamic vertical force, Fig. 7 the amplitude of the first harmonic and Fig. 8 the amplitude of the second harmonic of the vertical force. The model shows an excellent agreement with Wu's results for small amplitudes of motion. For the first frequency ($kR = 0.1$), the mean vertical force and the first and second harmonics increase with the amplitude of motion. At higher frequency ($kR = 10$), only the second harmonic is a growing function of the amplitude (Fig. 8) and the mean vertical force is negative (Fig. 6). Beyond $B/R = 1$, the cylinder is moving close to the free surface and nonlinear effects play a significant role. This might explain the discrepancy with Wu's theory for larger amplitudes of motion.

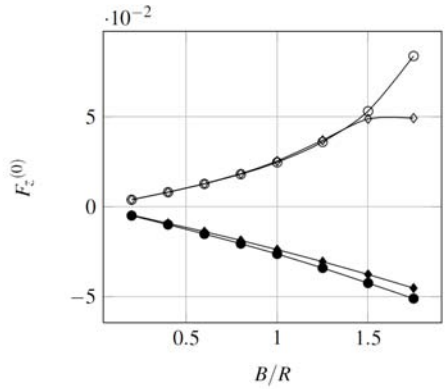

Figure 6: Mean non-dimensional vertical force $F_z^{(0)}$ with $kR = 0.1$ (—◇—) and $kR = 1.0$ (—◆—), compared to Wu's (1993) analytical theory (—○—,—●—).

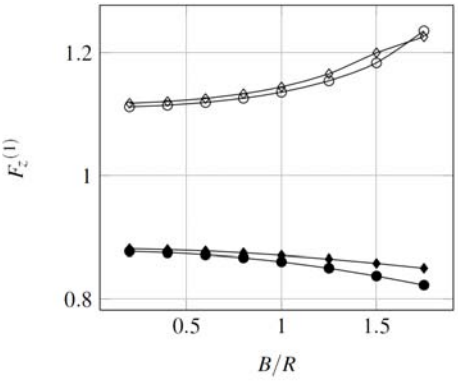

Figure 7: 1st harmonic amplitude of the vertical force $F_z^{(1)}$ with $kR = 0.1$ (—◇—) and $kR = 1.0$ (—◆—), compared to Wu's (1993) analytical theory (—○—,—●—).

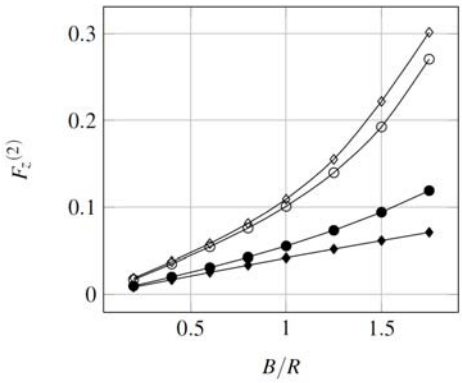

Figure 8: 2nd harmonic amplitude of the vertical force $F_z^{(2)}$ with $kR = 0.1$ (—◇—) and $kR = 1.0$ (—◇—), compared to Wu's (1993) analytical theory (—○—,—●—).

Cylinder in a Prescribed Clockwise Circular Motion

Another interesting case treated by Wu (1993) is that of a horizontal circular cylinder in a large-amplitude circular motion. Wu computed the harmonics of the vertical and horizontal hydrodynamic forces for different amplitudes of motion, and one frequency ($kR = 0.5$). Starting from a free surface at rest, waves are generated only in the rightward direction (Fig. 9), for a clockwise motion of the cylinder.

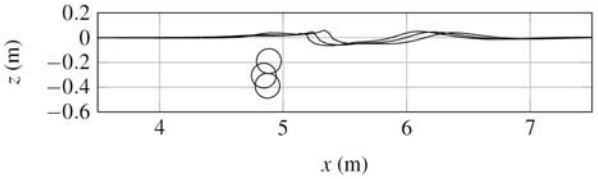

Figure 9: Successive snapshots ($t/T = 4.40, t/T = 4.49, t/T = 4.62$) of waves generated by the clockwise circular motion of a cylinder ($A/R = 1.75, kR = 0.5$)

Numerical simulations were performed in a flume of water depth $d = 3$ m and length $L = 20$ m, with an absorbing beach over the last 7 m. A cylinder of radius $R = 0.1$ m is placed at 5 m away from the left boundary and $z_c = -3R$ under the undisturbed free surface and is moved on a circular path with a rotational speed ω and radius C. The hypothesis of infinite depth made by Wu is verified in our simulations, with $kd = 5$. Like for the purely vertical motion, in the BEM, 200 nodes are used on the free surface and 80 on the cylinder; here, simulations lasted for about 15 periods.

The mean non-dimensional forces are plotted in Fig. 11, while the first and second harmonics of these forces are shown in Fig. 12 and Fig. 13. These figures show a good agreement with Wu's results for amplitudes of motion below $C/R = 1$. Nonlinear effects play a significant role beyond this limit, as shown on the vertical force (Fig. 10).

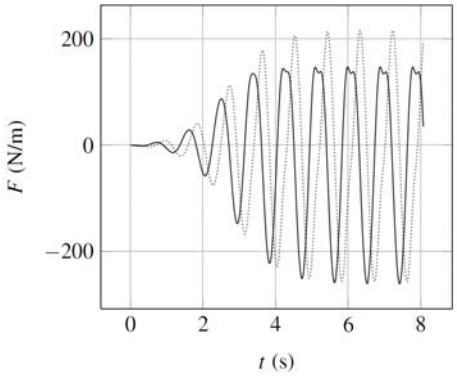

Figure 10: Vertical (——) and horizontal (·····) hydrodynamic forces exerted on the cylinder - $kR = 0.5$ and $C/R = 1.75$

Kent and Choi (2007) also compared results of their NWT based on the HOS method to Wu's analytical results. Unfortunately they did not go beyond a $C/R = 0.6$ amplitude of motion, for which nonlinear effects do not clearly manifest themselves.

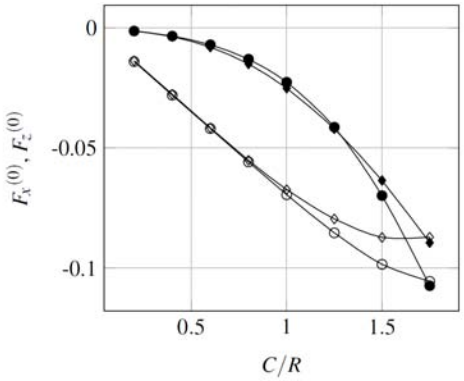

Figure 11: Mean non-dimensional vertical (—♦—) and horizontal (—◇—) forces with $kR = 0.5$, compared to Wu's (1993) analytical theory (—●—,—○—).

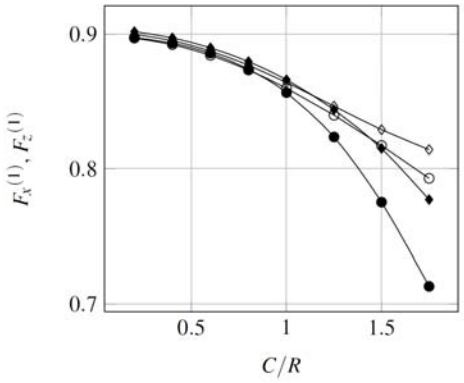

Figure 12: 1st harmonic amplitude of the non-dimensional vertical (—♦—) and horizontal (—◇—) forces with $kR = 0.5$, compared to Wu's (1993) analytical theory (—●—,—○—).

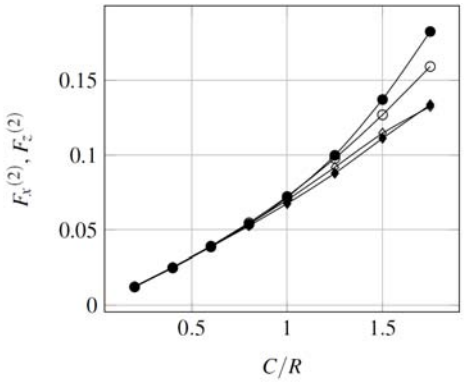

Figure 13: 2nd harmonic amplitude of the non-dimensional vertical (—♦—) and horizontal (—◇—) forces with $kR = 0.5$, compared to Wu's (1993) analytical theory (—●—,—○—).

A SUBMERGED CYLINDER IN FREE MOTION

In the previous section, we verified that our model reproduced the well-known property that a submerged cylinder undergoing forced circular motion acts as a unidirectional wavemaker. By reversing this process, one might easily envision that, in a wave field, a cylinder suitably constrained by anchors and power take-off systems (e.g., represented by equivalent springs and dash pots), would act as an efficient wave energy absorber, that would have the potential to become an element of a Wave Energy Converter (WEC). Quite a large body or research, in fact, exists along these lines, which focuses on harnessing wave power based on oscillating/rotating submerged bodies. One famous example is the so-called "Bristol cylinder", introduced and studied in the 1980s (e.g., Evans et al., 1979), which will serve as a more demanding and realistic test case of our model. Hence, we consider the motion of a submerged circular cylinder, under regular waves, and compare our numerical results to the first-order (linear) solution by Evans et al. (1979). Assuming a mass M per unit length, the wave-induced motion $\mathbf{x}$ of the cylinder center of mass, from its initial resting position $\mathbf{x_{ini}}$, is governed by:

$$M\ddot{\mathbf{x}} = \mathbf{F_h} - Mg\underline{\mathbf{z}} - d_0\dot{\mathbf{x}} - k_0(\mathbf{x} - \mathbf{x_{ini}}) \tag{20}$$

where $\mathbf{F_h}$ is the wave-induced hydrodynamic force and (k_0, d_0) are spring stiffness and damping constant, respectively, selected identical in x and z directions, and specified as a function of a "tuning" angular frequency $\omega_0 = 2\pi f_0$ as:

$$k_0 = \{M + a_{ii}(\omega_0)\}\,\omega_0^2 \tag{21}$$

$$d_0 = b_{ii}(\omega_0) \tag{22}$$

where $a_{ii}(\omega_0)$ and $b_{ii}(\omega_0)$ the (linear) added mass and wave radiative damping of the submerged cylinder, respectively, at the tuning frequency. Evans et al. (1979) showed that, under those conditions and within the linear approximation, the tuned cylinder describes a circle of radius C under the action of regular waves of angular frequency ω and amplitude A:

$$\left(\frac{C}{A}\right)^2 = \frac{\rho g^2 b_{ii}(\omega)}{\omega^3\left\{(d_0 + b_{ii}(\omega))^2 + \frac{1}{\omega^2}[k_0 - (M + a_{ii}(\omega))\omega^2]^2\right\}} \tag{23}$$

where $a_{ii}(\omega)$ and $b_{ii}(\omega)$ are the (linear) added-mass and the wave radiative damping at frequency ω, respectively.

We simulate one of the configurations studied by Evans et al. (1979), namely a neutrally buoyant circular cylinder of radius $R = 0.05$ m, whose center is initially at a submergence depth $z_c = -0.0625$ m (i.e., there is 1.25 cm of water on top of the cylinder), in depth $d = 0.60$ m.

The "tuning" frequency is $f_0 = 1.65$ Hz. In order to favorably compare model results with those of the linear theory, we use the lowest wave amplitude used by Evans et al., namely $A/R = 0.033$, and successively run the model for 8 incident wave frequencies, over the interval [1 Hz ; 2 Hz].

Fig. 14 shows the simulated cylinder trajectory, for one of the selected frequencies. Once steady-state is reached, after a ramp-up period from the initial state of rest, the cylinder center of mass follows a nearly circular pathline (shown in the figure). This circular motion remains stable thereafter. This behavior is also observed for all other frequencies. Fig. 15 shows results for the radius of circular motion (made non-dimensional by the wave amplitude A), as a function of kR, compared to predictions from Evans et al.'s (1979) linear theory. The simulated values are quite close to the predictions, although the calculated "radius" is somewhat smaller than the theoretical one. This could be due to nonlinear effects due to the cylinder shallowness of submergence.

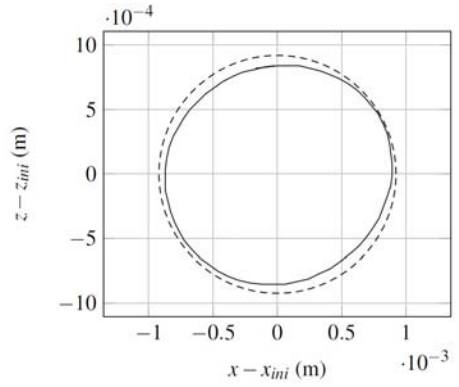

Figure 14: Path of the center of mass (——) of the tuned cylinder (at $f_0 = 1.65$ Hz) over one period (case $f = 1.5$ Hz, $kR = 0.45$) compared to the circular path predicted by Evans et al.'s linear theory (1979) (- - - -).

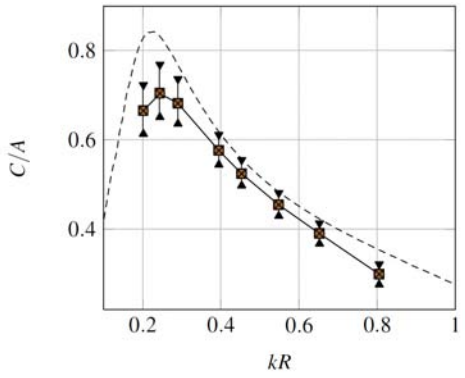

Figure 15: Radius of the circular path of the center of mass: linear theory by Evans et al. (1979) (- - - -). The tuning frequency corresponds to $kR = 0.55$. Symbols refer to the minimum, average and maximum values of the simulated path over one period.

Overall, this application confirms the ability of our model to simulate large wave-induced motions of "freely-moving" submerged bodies. This also represents a first realistic application on the way to model the dynamics of submerged WECs, which is the long term goal of the present research project.

CONCLUSION

A 2D FNPF numerical wave model was extended to include a submerged horizontal cylinder, of arbitrary cross-section. The mathematical problem was formulated and then numerically solved for two situations corresponding to a body with prescribed motion (including the case of a fixed body) and a freely-moving body. In the latter case an exact coupling strategy (which hence does not require iterations) was implemented, based on the implicit BIE method proposed by Van Daalen (1993) and Tanizawa (1995). In our

implementation of this method, the dynamical equations of body motion were marched in time with a Newmark scheme. The model was applied and validated for various cases, including a fixed circular cylinder beneath waves (experiments by Chaplin, 1984), the forced motion of a cylinder, either in vertical oscillations or circular motion (with comparison to the theoretical results of Wu, 1993). In all of these validation applications the model performed at least as well as earlier proposed solutions. Finally a preliminary application to a freely-moving cylinder, representing an idealized WEC, was presented, with comparison to results of a linear model.

The validation of the coupled model for more realistic cases is ongoing, including applying it to irregular waves, in order to study the effects of sea-sate parameters (period, significant wave height, spectral bandwidth, composite spectra) on the dynamics of the submerged body. The model will then be extended to 3D cases, for which the wave model is already at hand (e.g., Grilli et al., 2001; Sung and Grilli, 2008).

REFERENCES

Cao, Y, Beck, RF, and Schultz, WW (1994). "Nonlinear Computation of Wave Loads and Motions of Floating Bodies in Incident Waves," *Proc 9th (1994) Int Workshop on Water Waves and Floating Bodies*, Kuju, Oita, Japan.

Chaplin, JR (1984). "Nonlinear Forces on a Horizontal Cylinder Beneath Waves," *J Fluid Mech*, Vol 147, pp 449-464.

Clément, A (1996) "Coupling of Two Absorbing Boundary Conditions for 2D Time-domain Simulations of Free Surface Gravity Waves," *J Comp Phys*, Vol 126, No 1, pp 139-151.

Cointe, R (1989). "Quelques aspects de la simulation numérique d'un canal à houle". Thèse de Doctorat, Ecole Nationale des Ponts et Chaussées, France (in French).

Dean, WR (1948). "On the Reflexion of Surface Waves by a Submerged Circular Cylinder," *Proc Camb Phil Soc*, Vol 44, pp 483-491.

Evans, DV, Jeffrey, DC, Salter, SH, and Taylor, JRM (1979). "Submerged Cylinder Wave Energy Device: theory and experiment," *Applied Ocean Research*, Vol 1, No 1, pp 3-12.

Fox, L, and Goodwin, ET (1949). "Some New Methods for the Numerical Integration of Ordinary Differential Equations," *Math Proc Camb Phil Soc*, Vol 45, pp 373-388.

Greenhow, M, and Ahn, SI (1988). "Added Mass and Damping of Horizontal Circular Cylinder Sections," *Ocean Eng*, Vol 15, No 5, pp 495-507.

Grilli, ST (1997). "Fully Nonlinear Potential Flow Models used for Long Wave Runup Prediction." Chapter in "Long-Wave Runup Models", (eds. H. Yeh, P. Liu, and C. Synolakis), pps. 116-180. World Scientific Publishing, Singapore.

Grilli, ST, Guyenne, P, and Dias, F (2001). "A fully Nonlinear Model for 3-D Overturning Waves over an Arbitrary Bottom," *Int J Numer Meth Fluids*, Vol 35, pp 829-867.

Grilli, ST, and Horrillo, J (1997). "Numerical Generation and Absorption of Fully Nonlinear Periodic Waves," *J Eng Mech*, Vol 123, No 10, pp 1060-1069.

Grilli, ST, Skourup, J, and Svendsen, IA (1989). "An Efficient Boundary Element Method for Nonlinear Water Waves," *Eng Analysis with Boundary Elements*, Vol 6, No 2, pp 97-107.

Grilli, ST, and Subramanya, R (1994). "Quasi-singular Integrations in the Modelling of Nonlinear Water Waves," *Eng Analysis with Boundary Elements*, Vol 13, No 2, pp 181-191.

Grilli, ST, and Subramanya, R (1996). "Numerical Modeling of Wave Breaking Induced by Fixed or Moving Boundaries". *Computational Mechanics*, Vol 17, No 6, pp 374-391.

Grilli, ST, and Svendsen, IA (1990). "Corner Problems and Global Accuracy in the Boundary Element Solution of Nonlinear Wave Flows," *Eng Analysis with Boundary Elements*, Vol 7, No 4, pp 178-195.

Grue, J, and Granlund, K (1988). "Impact of Nonlinearity upon Waves Traveling Over a Submerged Cylinder," *Proc 3rd (1988) Int Workshop on WaterWaves and Floating Bodies*,Woods Hole, MA, USA.

Kent, CP, and Choi, W (2007). "An Explicit Formulation for the Evolution of Nonlinear Surface Waves Interacting with a Submerged Body," *Int J Numer Meth Fluids*, Vol 55, pp 1019-1038.

Koo, W, and Kim, MH (2004). "Freely-floating Body by a 2D Fully Nonlinear Numerical Wave Tank," *Ocean Eng*, Vol 31, pp 2011-2046.

Liu, Y, Dommermuth, DG, Yue, DKP (1992). "A High-Order Spectral Method for Nonlinear Wave-Body Interactions," *J Fluid Mech*, Vol 245, pp 115-136.

Mann, LD, Burns, AR, and Ottaviano, ME (2007). "CETO, a Carbon Free Wave Power Energy Provider of the Future," *Proc 7th (2007) European Wave and Tidal Energy Conference*, Porto, Portugal.

Ogilvie, TF (1963). "First- and Second-Order Forces on a Cylinder Submerged Under a Free Surface," *J Fluid Mech*, Vol 16, pp 451-472.

Sen, D (1993). "Numerical simulation of motions of two-dimensional floating bodies," *J Ship Research*, Vol 37, No 4, pp 307-330.

Sung, HG, and Grilli, ST (2008). "BEM Computations of 3-D Fully Nonlinear Free-Surface Flows caused by Advancing Surface Disturbances," *Int J Offshore and Polar Eng*, ISOPE, Vol 18, No 4, pp 292-301.

Tanizawa, K (1995). "A Nonlinear Simulation Method of 3D Body Motions in Waves, 1st Report" *J Soc Naval Arch Japan*, Vol 178, pp 179-191.

Tavassoli, A, and Kim, MH (2001). "Interactions of Fully Nonlinear Waves with Submerged Bodies by a 2D Viscous NWT," *11th (2001) Int Offshore and Polar Eng Conf*, Stavanger, Norway, ISOPE, Vol 3, pp 348-354.

Ursell, F (1949). "Surface Waves in the Presence of a Submerged Circular Cylinder, I and II," *Proc Camb Phil Soc*, Vol 46, pp 141-158.

Van Daalen, EFG (1993). "Numerical and Theoretical Studies ofWater Waves and Floating Bodies". PhD Thesis, University of Twente, The Netherlands.

Vinje, T, and Brevig, P (1981). "Nonlinear, Two-Dimensional Ship Motions," *Norwegian Institute of Technology*, Report R-112.81.

Wu, GX (1993). "Hydrodynamic Forces on a Submerged Circular Cylinder Undergoing Large-amplitude Motion," *J Fluid Mech*, Vol 254, pp 41-58.

Wu, GX, and Eatock-Taylor, R (1996). "Transient Motion of a Floating Body in Steep Water Waves," *Proc 11th (1996) Int Workshop on Water Waves and Floating Bodies*, Hamburg, Germany.